Journal of Materials Chemistry B

Accepted Manuscript

ROYAL SOCIETY OF CHEMISTRY

www.rsc.org/materialsB

Facile and Rapid Ruthenium Mediated Photo-crosslinking of Bombyx mori Silk Fibroin

Jasmin L. Whittaker, [a]Namita R. Choudhury,[a] Naba K. Dutta[a]* and Andrew Zannettino[b]*

[a]Ian Wark Research Institute,

University of South Australia, Mawson Lakes, Adelaide, SA 5095, Australia

[b]Myeloma Research Laboratory, School of Medical Sciences,

University of Adelaide, Adelaide, SA, Australia.

* Prof. Namita R. Choudhury

E-mail: namita.choudhury@unisa.edu.au, Tel.: +61883023719

* Prof. Naba K. Dutta

E-mail: naba.dutta@unisa.edu.au, Tel.: +61883023546

Abstract

A facile and rapid ruthenium catalysed photo-crosslinking method was employed to prepare *Bombyx mori* silk fibroin hydrogels for the first time that may be used for biomedical applications. The gels have been characterised by differential scanning calorimetry (DSC), dynamic mechanical analysis (DMA), photo-acoustic fourier transform infrared spectroscopy (PA-FTIR), and x-ray diffraction (XRD). We have reported the tuning of the properties of the chemically crosslinked gels through hydration level. DSC and DMA measurements have shown that the molecular chain dynamics and mechanical properties are dependent on the moisture/water content. The structural changes upon gelation were examined through the use of DSC, PA-FTIR and XRD, which confirmed that the gels contained less crystalline component than the original silk powder. Finally, the biocompatibility and hence, potential tissue engineering application of the silk fibroin hydrogel was also assessed by culturing chondrocyte progenitor cells for up to one week on the engineered fibroin surfaces.

Keywords

protein-polymers; elastomers; hydrogels; silk fibroin

Introduction

Hydrogels are three-dimensional, insoluble structures composed of physically or chemically crosslinked materials and find applications in the field of regenerative medicine/tissue engineering.[1] The design requirements for scaffolds are extensive and include biocompatibility, mechanical integrity, controlled degradability, cell signaling, etc. Also, tissue stiffness plays a central role in the adhesion and cytoskeletal organisation by acting as an informational template to the cells. Therefore, it is important to engineer the environment of the scaffolds by tuning their properties. One method to enhance the strength of gels is through crosslinking. A number of different natural and synthetic polymers, including collagen, elastin, poly(acrylic acid) (PAA), and poly(vinyl alcohol) (PVA), among many others, have been used to form hydrogels. Due to its superior strength, biocompatibility, biodegradability, and good oxygen and water vapour permeability, *Bombyx mori* (*B. Mori*) silk fibroin has excellent potential for biomedical materials development.[2,3] In addition, the processing methods related to silk fibroin are flexible in that an aqueous or organic solvent may be used.[4] As a result, silk fibroin has been investigated with regard to applications for tissue engineered blood vessels, skin, bone, and cartilage.[5]

In order to improve the strength, *B. mori* silk fibroin has been crosslinked via a number of methods in recent years. Physically crosslinked silk fibroin hydrogels have been produced through the induction of beta-sheet structure in silk fibroin solutions.[6] A number of different parameters can result in the sol-gel transition of silk fibroin through the formation of beta-sheet stabilised structures. These have been studied extensively and include: shearing, water evaporation, heating, solvent exposure, low pH, high ionic strength, and electric current.[6-10] Chemically crosslinked silk fibroin hydrogels have also been studied, however to a lesser extent. Vasconcelos et al. employed the natural covalent crosslinking agent genipin to form solid structures.[11] In a study by Liu et al., silk fibroin was crosslinked by first performing

ultrasonication to induce gelation through beta-sheet formation. Following this, the silk was chemically crosslinked using genipin. The advantage of using a natural crosslinking agent such as genipin, is reduced cytotoxicity when compared to synthetic crosslinkers, such as glutaraldehyde.[11] However, the use of genipin as a crosslinker is time consuming and requires 6 hours to achieve maximum crosslinking.[11] This is due to the fact that it has been reported that genipin reacts mainly with lysine and arginine in protein structures.[12] The lysine and arginine amino acids make up a low percentage of the total silk fibroin composition with approximately 0.6 mol% for each.[12] The enzymatic covalent crosslinking of silk fibroin using tyrosinase was reported by Kang et al.[13] This reaction was also time consuming, with approximately 20 hours required.[13] Therefore, it would be extremely important and useful to identify a facile and rapid crosslinking method to develop chemically crosslinked silk fibroin gels.

In our earlier work, a recombinant form of the elastic protein resilin, rec1-resilin, was photo-dynamically crosslinked using tris(2,2'-bipyridyl)dichlororuthenium(II) as the catalyst and ammonium peroxodisulfate as the electron acceptor.[14] In this method, the tyrosine residues in the protein structure were employed to form di-tyrosine crosslinks. Stable rec1-resilin gels with tuneable crosslink densities and mechanical properties were achieved. Recently, Schacht and Scheibel used this method to photo-chemically crosslink a recombinant spider silk protein.[15] *B. mori* silk fibroin contains 4.98 mol% of tyrosine in its overall structure, which is slightly less than that of the recombinant resilin protein.[16] Therefore, it is hypothesised that this method will provide a rapid and simple process for crosslinking of *B. mori* silk fibroin.[4] Successful achievement in the processing of *B. mori* silk fibroin gels via this method would increase its uses in a range of applications and provide opportunities for conjugation with other materials. It has been confirmed that ruthenium and APS concentrations used for this method of crosslinking are

not cytotoxic and thus this method could be employed for in situ crosslinking through a photodynamic approach, increasing its uses for different applications.[17]

In this study, silk fibroin solutions were photo-dynamically crosslinked to form gels through covalent interactions between tyrosine residues. The physical properties, including crosslink density, of these gels were determined using water uptake studies. The structural characteristics of the gels were investigated using Fourier transform infrared (FTIR) spectroscopy and differential scanning calorimetry (DSC). The mechanical properties of the gels were studied under different humidity levels using dynamic mechanical analysis (DMA). Finally, the biocompatibility of the silk fibroin hydrogels was demonstrated through cell culture studies using a pre-chondrocyte cell line, ATDC5. This method provides a basis for simple crosslinking of silk fibroin for the creation of more complex biomaterials with tuneable moduli through chemical crosslinking with other systems.

Experimental

Silk fibroin

Bombyx mori silk was purchased as raw silk from Beautiful Silks, Australia from which silk fibroin was regenerated. Also, water-soluble (BMWS) freeze dried regenerated silk fibroin powder was given by Dr. Anja Glisovic, Germany. The structural components of the silk fibroin from the raw silk and BMWS powder have been confirmed through nuclear magnetic resonance (NMR) (Supporting Information S1).

Solution preparation

The raw silk was degummed by boiling in aqueous 0.02 M Na_2CO_3 for 30 minutes. The silk was rinsed in distilled water three times and allowed to dry at room temperature overnight. The fibroin was then dissolved in a calcium chloride, water, ethanol solution ($CaCl_2/H_2O$/EtOH 1/8/2 molar ratio), with a liquor ratio of 1:10, at 70 ^oC for 24 hours. Following this, the solution was

cooled and filtered using non-sterile pre-filter (Minisart-GF 17824) with a pore size of approximately 1.2 microns. The concentration of the silk fibroin in the solution was determined to be approximately 140 mg/mL.

Solutions of BMWS silk fibroin of varying concentrations were prepared by slowly adding the silk fibroin powder to distilled water (DW) whilst sonicating (Table 1). Sonication was conducted for less than one hour to prevent beta-sheet formation. The solution was filtered using a non-sterile pre-filter (Minisart-GF 17824) with a pore size of approximately 1.2 microns.

All silk fibroin solutions were stored at 4 ^{o}C to prevent silk fibroin gelation.

Table 1. Water uptake and crosslink density values of gels under different conditions.

Sample	Silk fibroin (mg/mL)	$Ru(II)(bpy)_3^{2+}$ (mM)	Molar ratio $Ru(II)(bpy)_3^{2+}$: APS	Q (swelling ratio)	h (water uptake)	$v_e \times 10^{-3}$ (mol/cm^3)
Ru0.16APS20	300	0.16	1:125	1.64	0.638	0.374
Ru0.5APS20	300	0.5	1:40	1.54	0.538	0.380
Ru1APS20	300	1	1:20	1.59	0.592	0.377
Ru5APS20	300	5	1:4	1.57	0.574	0.378
Ru10APS20	300	10	1:2	1.59	0.589	0.377
Ru5APS28	300	5	1:5.6	1.60	0.599	0.376
Regenerated SF solution	140	5	1:5.6	1.64	0.636	0.374
Ru5APS100	300	5	1:20	1.59	0.587	0.377
BMWS150	150	5	1:5.6	1.61	0.606	0.376

Photochemical crosslinking

Table 1 shows the various compositions that are used for photochemical crosslinking of regenerated silk solution and solution made from BMWS at different concentration. An aqueous silk fibroin solution was photo-chemically crosslinked to form a gel, using Tris(2,2-bipyridyl)

dichloro ruthenium (II) hexahydrate ($Ru(II)(bpy)_3^{2+}$) as the catalyst and ammonium persulphate (APS) as the electron acceptor (see Figure S2 for full reaction schematic). Predefined amounts of $Ru(II)(bpy)_3^{2+}$, APS, and silk fibroin solution were mixed, whilst preventing exposure to light (Table 1). The solutions were then transferred to a teflon mould and exposed to a 250W light source for 120 seconds, and then the gels were turned over and exposed to the light source for a further 60 seconds to ensure full crosslinking of the sample (Figure 1). The mass of crosslinked gel was measured and the gel was subsequently immersed in distilled water (DW) for several days to remove the un-reacted material. The water was changed daily. Samples were prepared in duplicate. The gels were dried for three days in the fume hood at room temperature and subsequently for 3 hours in the vacuum oven at 40°C to a constant weight. The dry weight (w_d) and dimensions of the gels were measured using digital callipers. The BMWS dry and swollen gels were further examined by spectroscopic, thermal and X-ray analyses.

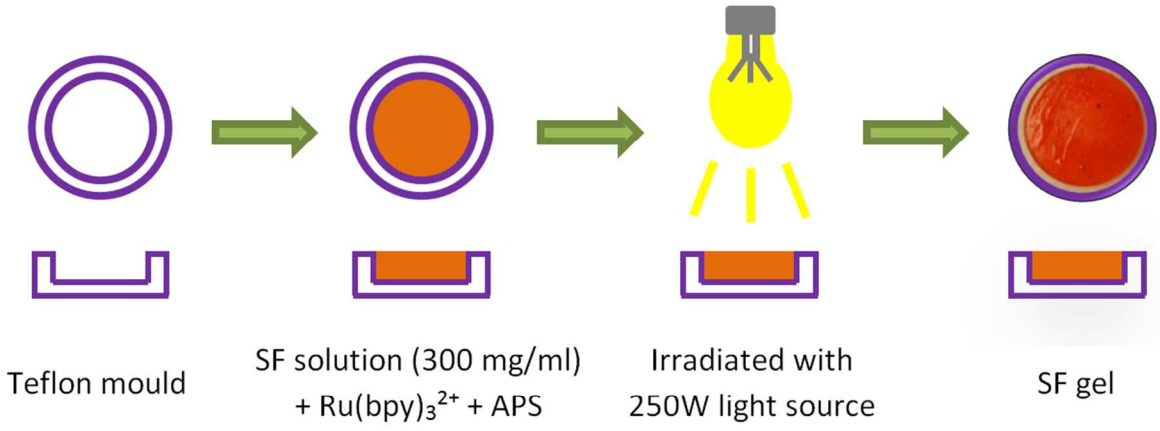

Figure 1. Method for photodynamic crosslinking of *B. mori* silk fibroin.

Water and water vapour uptake studies

For water uptake studies, the gels were immersed in DW and the weight was taken at different time intervals to monitor the water uptake and determine the equilibrium swelling weight (w_s).

Vapour sorption experiments were conducted by placing the gels in a controlled humidity chamber (ESPEC, SH-241 temperature & humidity chamber, Espec Corp., Japan) at specific conditions including temperature and percent relative humidity (%RH). The weight of the samples was monitored at different time intervals using an accurate microbalance capable of measuring four decimal places. The swelling ratio (Q) and water uptake (h) for the bulk water and water vapour uptake studies were determined using the equations 1 and 2.

$$Q = \frac{w_s}{w_d} \qquad (1)$$

$$h = \frac{w_s - w_d}{w_d} \qquad (2)$$

where, w_s is the weight of the swollen silk fibroin gel at varying time intervals and conditions, and w_d is the dry weight of the crosslinked silk fibroin gel.

Determination of crosslink density for silk fibroin gels

The crosslink densities of the gels were determined through equilibrium swelling experiments conducted in DW at room temperature. After drying, the gels were immersed in DW and the weight of the gel was monitored until the equilibrium weight ($w_{T,s}$) was reached. The crosslink density of the silk gel samples was calculated using equations 3 and 4.[14] The Flory-Huggins interaction parameter (χ) between silk fibroin and water was taken as 0.95.[18] The densities of the dry silk fibroin gel (ρ_P) and water at room temperature (ρ_2) are 1.421 g/cm^3 and 0.997 g/cm^3, respectively.[14,19] The molar volume of water (V_2) is 18 cm^3/mol.[14]

$$v_{1,s} = \frac{w_p/\rho_p}{\frac{w_{T,s}-w_p}{\rho_2}+w_p/\rho_p} \qquad (3)$$

$$v_e = \frac{\rho_p}{M_c} = \frac{-\ln(1-v_{1,s})+v_{1,s}+\chi v_{1,s}}{V_2(v_{1,s}-\frac{1}{2}v_{1,s})} \qquad (4)$$

Porosity of hydrogel from scanning electron microscopy (SEM)

The internal microstructure of the representative Ru5APS28 hydrogels was analysed using Environmental SEM (ESEM) with the Quanta FEG 450, FEI. The gels were immersed in DW until equilibrium swelling was reached. The hydrogels were cut to expose cross sections and were examined using ESEM mode under an accelerating voltage of 30 kV. The ESEM experiments were conducted with a pressure of 900 Pa, temperature of 2 ^{o}C, and at 100% humidity. The pore size and distribution was examined using the ImageJ software.

Glass transition behaviour of gel by differential scanning calorimetry (DSC)

DSC measurement of the representative Ru5APS28 (Table 1) gel prepared from BMWS silk fibroin powder was conducted using the TA Instruments Discovery DSC. The instrument was calibrated for baseline and cell constant prior to running the experiments. The samples were sealed in hermetic aluminium pans for use in the DSC experiment, and an empty pan was used as the reference. The temperature range of experiment was from -80 ^{o}C to 300 ^{o}C, with a heating rate of 10 ^{o}C/min and under a controlled nitrogen gas flow rate of 50 ml/min.

Mechanical properties of the silk fibroin gels by dynamic mechanical analysis

DMA was conducted on the Ru5APS28 sample using the TA Instruments Q800 DMA equipped with a humidity accessory. The storage and loss moduli of the sample were determined under controlled humidity. The samples of rectangular geometry were immersed in DW initially for 24 hours to reach equilibrium water uptake before clamping. Then the samples were mounted using the tension clamp and run at ambient temperature with an amplitude of 10 μm and a preload force of 0.010 N. The DMA run was conducted with the humidity ramped to 50 % and held for the duration of an hour with isothermal temperature. The sample weight was measured at the beginning and end of each run to determine the water content, which changed over time as the

sample dried. This was conducted for six consecutive runs as the sample continued to dry. The sample weights were correlated to the measured modulus values.

Structural analysis of silk fibroin gels

In order to investigate the chemical structure, infrared spectra of the silk fibroin powder, film, and representative gel were acquired using Nicolet Magna-IR Spectrometer 750 in photo-acoustic mode using a carbon black reference. The spectra were obtained in the range 400 to 4000 cm^{-1} and the data was processed via the Omnic computer program. The amide I region was selected for investigation as it is commonly used to elucidate the secondary structure components of silk fibroin as it corresponds to the C=O stretching bonds in the peptide backbone.[20,21,22] Curve deconvolution of this region was conducted to analyse the secondary structure content of the samples. This was done using the Magic Plot software by applying Gaussian curve fitting to the amide I region (1600 – 1700 cm^{-1}).

X-ray diffraction (XRD) was also employed to examine the structure of the silk fibroin powder, filtered film, and the Ru5APS28 gel from filtered solution. The experiments were performed with X-ray diffractometer (Scintag/Thermo-electron ARL X'Tra XRD) using Copper Kα radiation (1.542 Å). X-Ray tube was run at 40kv, 30mA. Scans were performed from 5 to 90° 2Θ in steps of 0.02° at a rate of 1.2°/min (1 second count per data point).

Assessment of ATDC5 cell adhesion and proliferation

The ability of the swollen hydrogel (Ru5APS28) to support adhesion and proliferation of ATDC5 pre-chondrocyte cells (Riken laboratories, Japan) was examined.[23,24] The dried hydrogel discs of 6 mm in diameter were sterilized in 70% ethanol for 2 hours followed by overnight drying. Following this, the gels were swollen in sterile phosphate buffered saline (PBS) to equilibrium swelling level for cell culture experiments. The sterilized, swollen gels were then transferred to individual wells of a 96 well plate (Corning, USA) in preparation for cell culture.

The ATDC5 cell line was culture expanded in Dulbecco's Modified Eagle Medium (DMEM) supplemented with10% fetal calf serum (FCS) as previously described.[25] Prior to seeding the cells onto the hydrogels and tissue culture plastic (TCP), the cells were detached with 0.05% trypsin, enumerated using a hemocytometer and the cell concentration adjusted so that each well received 12 x 10^4 cell/cm^2. After incubation for 3 hours, an inverted light microscope (Olympus) was used to assess initial attachment and adhesion. The cells were incubated overnight, washed with PBS several times to remove non-adherent cells, fixed with paraformaldehyde (4%) solution for 1 hour, washed with PBS, and finally immersed in PBS for imaging. Phase-contrast micrographs were captured on the Nikon Eclipse Ti microscope through a 10X objective and recorded with a Qi1 Monochrome camera. Proliferation of the ATDC5 cells on the Ru5APS28 hydrogel samples was quantified using the WST-1 assay as previously described.[26] Briefly, ATDC5 cells were seeded onto Ru5APS28 hydrogels and TCP controls at a concentration of 3 x 10^4 cells/cm^2. Cell proliferation was evaluated at day 1, 3, 5 and 7. All experiments were performed in triplicate and the results presented as mean ± standard deviation (SD). Data was analysed using a Two-way ANOVA with Sidak's multiple comparisons test. A p-value less than 0.05 was considered statistically significant.

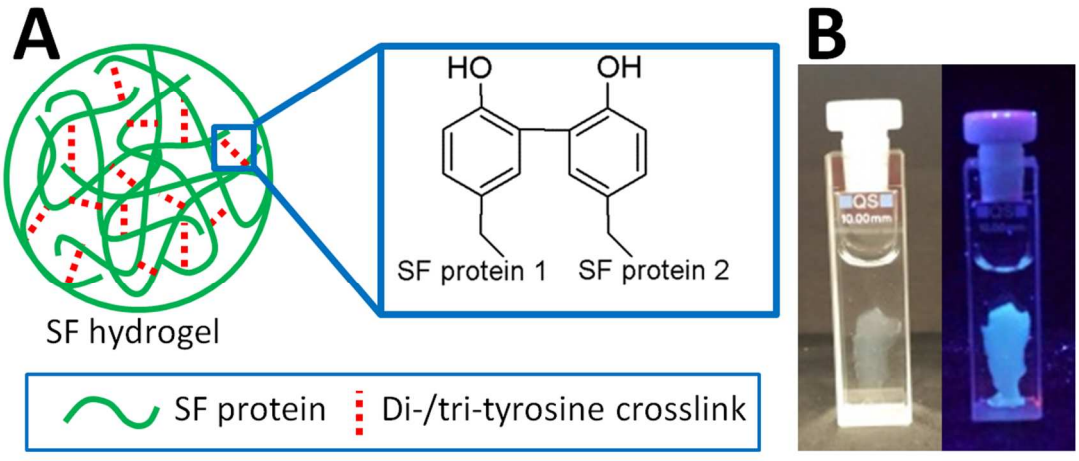

Figure 2. A) Schematic of crosslinked silk fibroin gel showing di-tyrosine crosslink. B) Photographs of a thin piece of photo-crosslinked silk fibroin under white and ultraviolet light.

Results and discussion

Photodynamic crosslinking

Photo-chemical crosslinking of *B. mori* silk fibroin with $Ru(II)(bpy)_3^{2+}$ catalyst was conducted using both regenerated silk fibroin solution and solution made from BMWS powder to study the versatility of the method (Table 1). In both cases, the formation of a solid gel structure was observed. The gel was brittle when dry and swelled macroscopically when exposed to aqueous environments. The structure of the gels is shown in Figure 2a, which shows the photo-induced crosslinking of silk through di-tyrosine links (see Figure S2 for full reaction mechanism).The nature of the di-tyrosine crosslinks have been confirmed through the fluorescence of an ultraviolet irradiated sample shown in Figure 2b (see Supporting Information S3 for fluorescence spectra). In addition, tri-tyrosine crosslinks are also possible, but cannot be distinguished from di-tyrosine in the fluorescence spectra. For a successful crosslinking reaction, a silk fibroin concentration of approximately 150 mg/ml or more was required. At a concentration of 150 mg/ml of BMWS, the gel was quite fragile and difficult to remove from the mould. In addition, the regenerated SF solution (~140 mg/mL) also formed a hydrogel; however this was also relatively fragile. Therefore, a concentration of ~300 mg/mL was deemed to be the optimum concentration for processing. Table 1 shows the conditions of crosslinking of the silk fibroin solution. The concentrations of the catalyst ($Ru(II)(bpy)_3^{2+}$) and electron acceptor (APS) were varied to understand the effect on the crosslink density and also to determine the effect of water swelling on the gel property. A minimum $Ru(II)(bpy)_3^{2+}$ concentration of 0.16 mM was required to obtain a gel that was strong enough to support itself when removed from the mould, however

the gel was quite fragile at this low $Ru(II)(bpy)_3^{2+}$ concentration (see Supporting Information S5). For ease of handling, a $Ru(II)(bpy)_3^{2+}$ concentration of 0.5 mM or greater was required. A sample of silk solution without $Ru(II)(bpy)_3^{2+}$ and APS was exposed to light and no gelation occurred, indicating the requirement of $Ru(II)(bpy)_3^{2+}$ and APS for successful crosslinking. This was also repeated individually with $Ru(II)(bpy)_3^{2+}$ and APS, where no gelation was observed. This observation certainly confirms the tyrosine mediated photodynamic crosslinking of fibroin solution, which has also been indicated through fluorescence and UV-vis spectroscopy measurements (see Supporting Information S3 and 4). Figure 3 shows optical photographs of the various BMWS silk fibroin gels at different stages of processing. The diameter of the gels reduced ~25% after leaching and ~60% of the initial diameter once fully dried. The average dimensions of the gels are also provided in Figure 3 and did not vary greatly between the different samples. There was a 10- to 12-fold decrease in the mass of the hydrogels from when they were formed to the dry gels, which was due to the loss of water and the unreacted silk fibroin, $Ru(II)(bpy)_3^{2+}$, and APS.

Water uptake (h) and crosslink density

Various silk gels prepared with different $Ru(II)(bpy)_3^{2+}$ and APS concentrations were investigated through water uptake studies to determine their effects on the crosslink density of the gels (Table 1). The equilibrium water uptake (h) value is a common measurement used to study the properties of proteins. In water immersion-sorption studies this value can be related to the crosslink density in that a lower absorption value is related to a highly crosslinked sample as it exists as a denser network. The values for the equilibrium water uptake of the BMWS gels were determined and varied minimally from 0.538 to 0.599 for the samples with $Ru(II)(bpy)_3^{2+}$ concentration greater than 0.5 mM, however the uptake was slightly higher (0.638) for the

sample with Ru(II)$(bpy)_3^{2+}$ concentration of 0.16 mM (Table 1). The water uptake curves for the gels were very similar with values close to each other and thus the water uptake of a representative sample (Ru5APS28) over time is shown (Figure 4A).

A comparison with rec1-resilin shows the level of water uptake to be quite low compared to the equilibrium h values reported for rec1-resilin gels, which were prepared through the same crosslinking method (ranged from approximately 2 to 4.5).[14] When protein gels are immersed in aqueous solutions, the water molecules initially interact with the polar residues followed by filling the voids. The water molecules interacting with the polar groups of the protein are non-crystallisable bound water molecules, whereas once these sites have been occupied, extra water present in the voids is crystallisable water.[14] In rec1-resilin, 46% of the residues are polar, whereas 19% are polar in silk fibroin.[14,16] Therefore, due to the significantly lower proportion of polar residues present in silk fibroins structure, it is not unexpected that the silk fibroin gels took up less water than the rec1-resilin gels.

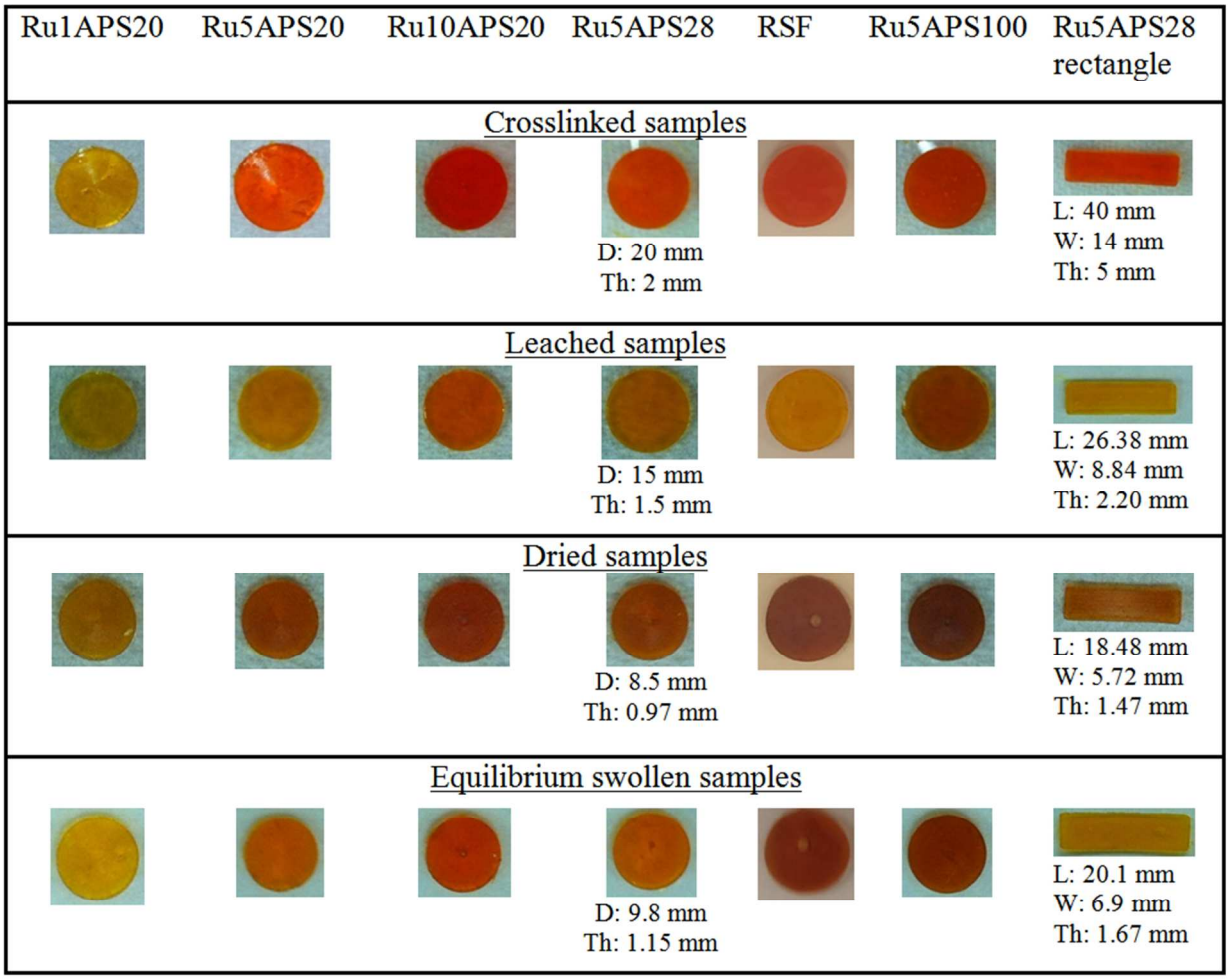

Figure 3. Photographs of silk fibroin gels from BMWS and regenerated SF (RSF) at different stages of processing. Sizes of round samples are average values at all different conditions as samples did not vary greatly in size. (D: diameter; Th: thickness; L: length; W: width)

The equilibrium water content was used to calculate the crosslink density of the gels prepared from different reactant concentrations, as described in our previous work.[14] The maximum crosslink density was determined to be 0.380 mol/cm^{3}and the conditions corresponding to this value were Ru(II)(bpy)$_3^{2+}$ and APS concentrations of 0.5 mM and 20 mM, respectively (Table 1). However, when the standard deviation for the sets of values was taken into account the crosslink did not vary with the different conditions. The exception to this was the sample with Ru(II)(bpy)$_3^{2+}$ concentration of 0.16 mM, which had a slightly lower crosslink density of 0.374

that did not overlap with the other values. Therefore, above a $Ru(II)(bpy)_3^{2+}$ concentration of 0.5 mM, the concentrations of the catalyst and electron acceptor did not have a significant effect on the crosslink density of the silk fibroin within the experimental range. Following this, the variables of crosslinking time, silk fibroin concentration, and interaction time of silk fibroin and reactants prior to crosslinking, were also investigated to determine their role in governing the crosslinking density. From the results in Table 1, it can be seen that the water uptake and crosslink density of the samples with extended crosslinking time, lower silk concentration, and a prolonged incubation time of reactants prior to exposure to light, had slightly higher values to the original gel at the same reactant concentrations (0.599). The values of water uptake were 0.620, 0.609, and 0.594 for the samples with less crosslinking time, lower silk fibroin concentration, and extended incubation time, respectively. However, when these values were used to calculate the crosslink densities, the values obtained were 0.375, 0.376, and 0.377 mol/cm^3, for less crosslinking time, lower protein concentration, and extended incubation time, respectively (Table 1). These crosslink densities were very similar to the original gel (Ru5APS28) prepared with the same $Ru(II)(bpy)_3^{2+}$ and APS concentrations (0.376 mol/cm^3). Thus, it is evident that these factors also did not markedly affect the crosslink density. When compared to the water uptake of the sample prepared at the same conditions using the regenerated silk fibroin solution (~140 mg/mL), the water uptake value (0.636) was slightly higher than the sample with a BMWS concentration of 150 mg/mL. This correlated to a crosslink density of 0.374 mol/cm^3, which matches closely with the data obtained for the BMWS gel with a similar concentration (0.376 mol/cm^3). This confirms that the ruthenium-mediated photo-crosslinking method is versatile and can be applied to silk fibroin solutions prepared from different methods.

When compared to other methods of silk fibroin crosslinking, the maximum crosslinking degree of genipin crosslinked silk fibroin with 24 hour reaction time was 29.4% as determined

by the ninhydrin assay.[11] In addition, the water uptake (h) of the genipin crosslinked silk fibroin scaffolds when immersed in aqueous solution was approximately 29 at neutral pH.[11] This is much higher than the water uptake for the photo-dynamically crosslinked silk fibroin gels (0.599). This observation indicates that our system has a higher crosslinking degree and less swelling was observed.

Considering the insignificant role of the above parameters, a representative photo-crosslinked silk fibroin sample (Ru5APS28) prepared from BMWS powder with intermediate condition of crosslinking was selected for further analysis of the chemical and physical properties.

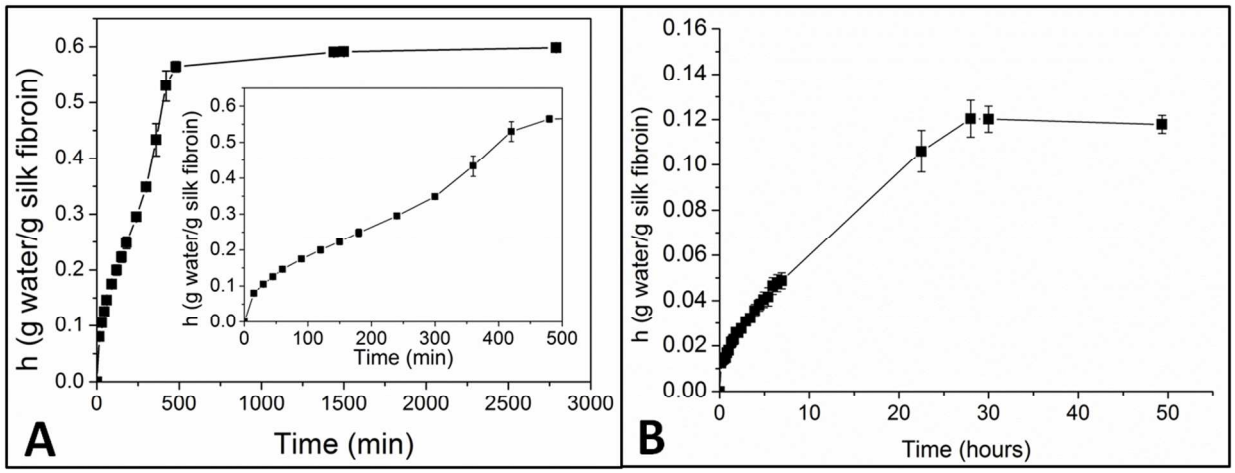

Figure 4. A) Plot of water uptake, h, as a function of time for sample Ru5APS28 when immersed in DW. Inset: shows initial water uptake to 500 minutes. B) Plot of water vapour uptake, h, with time for sample Ru5APS28 at T = 37°C and a_w = 0.9.

ESEM assessment of pore morphology of the silk fibroin hydrogels

The internal morphology of the representative Ru5APS29 hydrogels in the equilibrium-swollen state was examined on cross-sections of the hydrogels using ESEM. Figure 5 shows two different areas that highlighting the porous nature of the hydrogels. The average pore size was determined to be 2.49 ± 1.69 μm. In addition, the pore size distribution varied considerably,

ranging from 1.15 μm to 7.67 μm, a phenomenon observed with other silk fibroin hydrogel systems.[27] The pores were interconnected by larger flat areas, which aid in the impressive mechanical strength properties that the hydrogels exhibit.[11] The porosity of hydrogels in the swollen state is related to their water uptake capacity and rate of water uptake.[28,29] In comparison with other silk fibroin hydrogels[11,27], the hydrogels described here possess lower porosity (Figure 5), and this lower porosity correlates with the decreased capacity to take up water, as measured during the water uptake study. Thus, we have demonstrated that the silk fibroin hydrogels prepared by photodynamic crosslinking are porous in nature, which has important implication for their use in tissue engineering applications.[11]

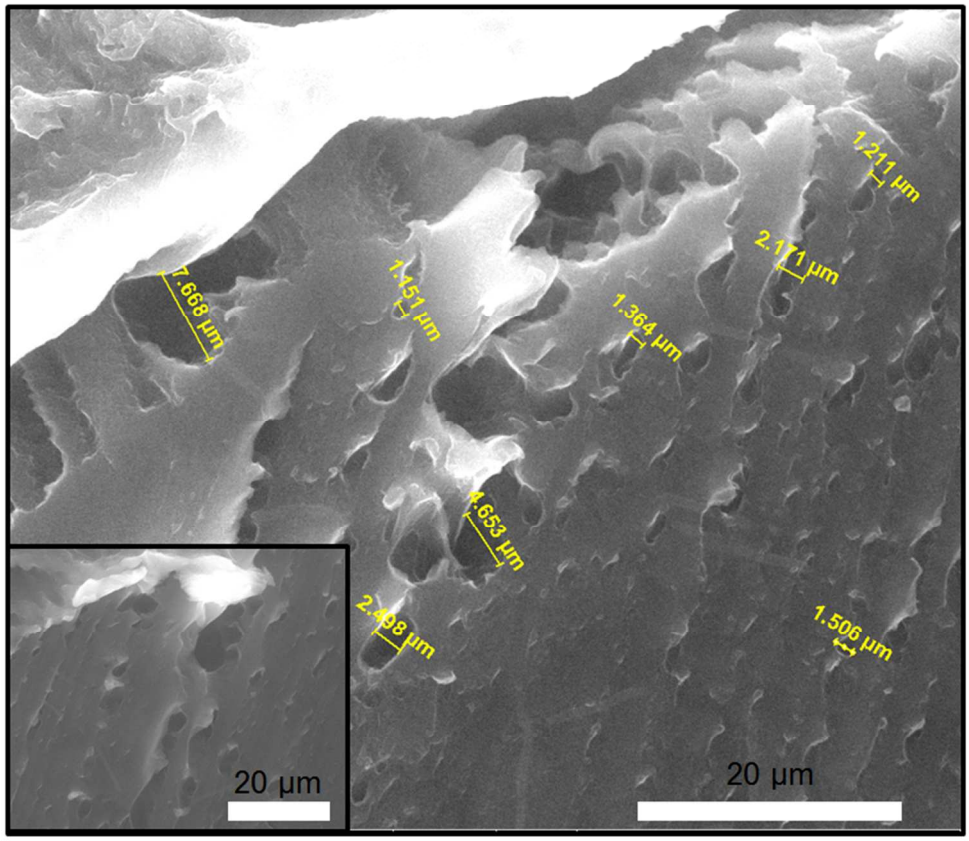

Figure 5. SEM image of two representative regions of the Ru5APS28 hydrogels showing pores size distribution.

Effect of hydration on the silk fibroin gel chain dynamics

DSC was used to measure the thermal behaviour of the silk fibroin powder, film and Ru5APS28 gel. Initially the glass transition temperatures (T_g) of the silk fibroin powder and filmwere determined and reported in Table 2. The dehydrated silk fibroin powder and the film show T_g values of 205 ^oC (the heat capacity change, ΔC_p = 0.47 J/g.^oC) and 158 ^oC (ΔC_p = 0.84 J/g.^oC), respectively. The film shows lowest Tg, which indicates the presence of amorphous silk fibroin with random coil conformation. On the other hand, the silk powder has less hydrophilic interaction and amorphous random coil conformation exhibiting a high T_g value characteristic of rigid structure.[30] However, from the Tg values it is clear that in both cases the intra- and intermolecular hydrogen bonds are broken leading to increased molecular motion. The change in heat capacity (ΔC_p) associated with the glass transition is a good indicator of the rigidity of the sample. In particular, Hu et al. have found a negative correlation between the ΔC_p and crystalline beta-sheet content of silk fibroin films.[30] The highest T_g value and lowest ΔC_p values of silk fibroin powder certainly reveals the presence of rigid β form of fibroin. This is attributed to the fact that during drying the powder has undergone thermally induced conformational transition from random coil to β form of fibroin. Moreover, it is evident that the silk solution contained predominantly the amorphous part of the silk as the film prepared from it exhibits lowest T_g and highest associated ΔC_p.

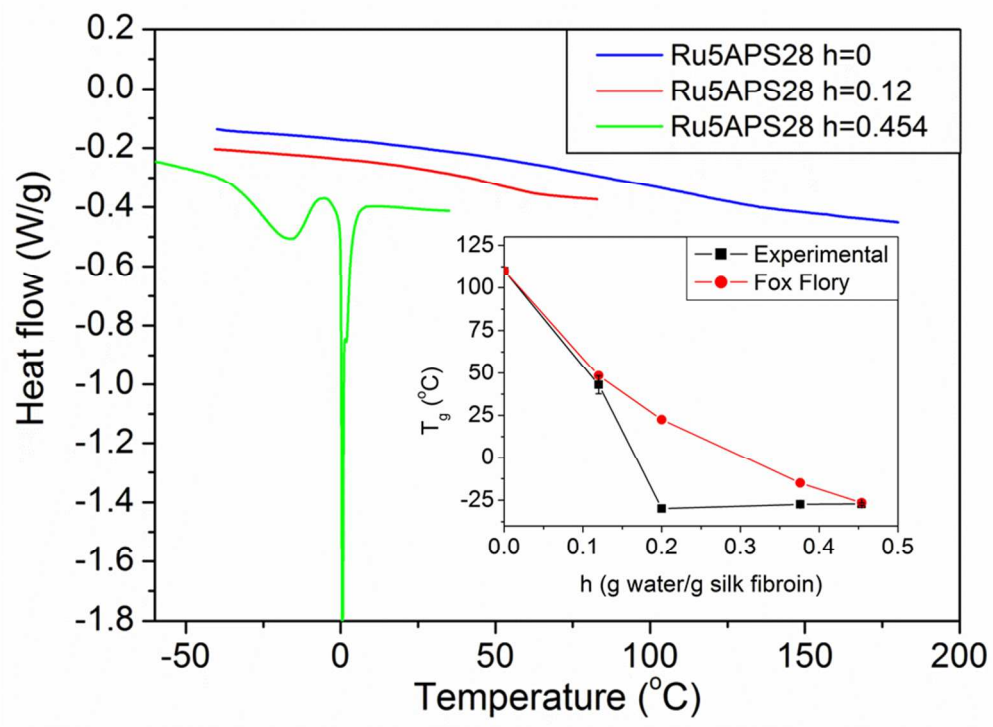

Figure 6. DSC thermograms of Ru5APS28 gel samples at different levels of hydration. Inset: comparison of experimental T_g to predicted Fox Flory values with different h values.

The DSC thermogram of the dehydrated Ru5APS28 gel displays two major thermal events: a shift of the baseline related to an increase in the specific heat capacity indicating the glass transition, and a more complex endothermic peak arising above 250°C due to chemical degradation of silk. Table 2 shows a summary of the T_gs of the Ru5APS28 gel under different hydration conditions. The dehydrated Ru5APS28 gel (h = 0) shows a glass transition temperature of approximately 110 °C (ΔC_p = 1.2 J/g.°C) (Figure 6). Thus, the thermal behaviour of the gel is significantly different from that of the film, and dry silk fibroin powder. When comparing the T_g value of the dried silk gel to the dried film (158 °C), the gel has a lower value and also a higher ΔC_p. This observation indicates that the film is more rigid in structure than the gel as more thermal energy is required for the glassy to plastic conversion. Therefore, the amorphous portion

of the silk solution comprised of more random coil form of fibroin took part in the crosslinking reaction. It is noteworthy that upon drying, the silk fibroin crosslinked gels become very brittle.

It is well known that moisture/water plays an important role in governing the chain dynamics and mechanical properties of the silk fibroin gel. Investigation into the behaviour of the gels when exposed to moisture/water gave us information about their stability, hydration capabilities, and the tuneability of the mechanical properties with different water uptake. The water vapour sorption was studied in addition to the immersion water uptake (h). The liquid water uptake and vapour sorption isotherms (37 ^{o}C and 90 %RH) for the crosslinked Ru5APS28 silk fibroin gel are shown in Figures 4A and 4B, respectively. The equilibrium h value for vapour sorption was determined to be 0.12 g water/g silk fibroin. In vapour sorption, water molecules were adsorbed and interacted with sites containing polar groups.[14] This is unlike immersion sorption where water also fills the voids after interacting with the polar groups. Therefore, as expected the water uptake was much less for vapour adsorption experiments. In addition, the equilibrium h value for the vapour sorption (0.12 g water/g silk fibroin) was lower than the value for the rec1-resilin gel at the same conditions which was approximately 0.25 g water/g rec1-resilin.[14] Our earlier work has shown that rec1-resilin gels, crosslinked through the same method, are highly elastic and resilient (>92%).[14] It has been reported that elastomeric proteins must exist in a hydrated or polar solvent environment in order to exhibit rubber-like elasticity.[31-33] This is because the internal chain dynamics and interactions of the proteins with water are responsible for the elasticity and resilience of the proteins.[34,35] The lowered propensity for the silk fibroin gels to take up moisture/water when compared to the rec1-resilins can thus be related to their differences in their structure, degree of hydrophobicity and hence resultant elasticity. Silk fibroin possesses a structure comprising of flexible and hydrophilic glycine residues (G-44.6 mol%) that alternate with rigid hydrophobic alanine residue (A-29.4mol%) based repeat units as represented by (-G-

A-G-A-G-S-) along with a variety of other amino acids, the most abundant of which are Serine (S-12 mol%), Tyr (Y-4.98 mol%), Asp (D), Arg (R) etc. Depending on the conformational transition and processing conditions, the tyrosine residue could either be buried with its phenolic hydroxyl group being a strong hydrogen bond donor, or the tyrosine group is exposed to surface in aqueous solution with its phenolic hydroxyl group being both donor and acceptor. Therefore, although rec1-resilin and silk have some common features, silk differs significantly in the fact that the overall structure is hydrophobic, whereas rec1-resilin is predominantly hydrophilic.

Table 2. T_g and ΔC_p values of BMWS silk fibroin samples at different conditions.

Sample	Processing conditions	h (g water/g silk fibroin)	T_g (^oC)	ΔC_p(J/g.^oC)
Powder	dehydrated	0	205	0.47
Un-crosslinked filtered film	dehydrated	0	158.3	0.84
Ru5APS28	dehydrated	0	110	1.2
Ru5APS28	equilibrium vapour sorption	0.12	43	-
Ru5APS28	liquid water uptake	0.454	-27.2	-

DSC was used to study the effect of hydration on the molecular dynamics of the Ru5APS28 silk fibroin gel samples. The DSC thermogram showed a dramatic change in the T_g of the Ru5APS28 silk fibroin gel to 43 ^oC for the sample at equilibrium vapour sorption (h = 0.12) under the conditions of 90 %RH at 37 ^oC (Figure 6). When the protein gel was in the dehydrated state, the intermolecular interactions were strong, and high temperatures were required for cooperative segmental motions (higher T_g).[14] However, in the presence of water, alternate hydrogen bonding donors and acceptors were available which results in a decrease in the energy barrier required for the plasticization of the system, and thus a lower T_g was exhibited.[14] The

effect of water on the T_g has also been reported for silk fibroin films, with a systematic decrease in T_g as the relative humidity increased.[36] The absence of an endothermic peak centred at 0 ^oC related to the melting of bulk water, confirmed that the water uptake at the equilibrium vapour sorption state is bound non-crystallisable water. Thus, the presence of non-crystallisable water was shown to act as a plasticizer for the silk fibroin gel system.

The thermal behaviour of the Ru5APS28 silk fibroin gel under immersion sorption conditions (h = 0.454) was also examined (Figure 6). The existence of an endothermic peak centred at 0 ^oC that remained with thermal cycling was due to the melting of bulk crystallisable water in the system. The T_g of the silk fibroin gel at this condition was observed at -27 ^oC. Thus at room temperature, the protein gel was in a flexible state.

The amount of crystallisable and non-crystallisable water was quantified using the endothermic melting of water in the DSC thermograms of Ru5APS28 samples under immersion sorption conditions. The amount of water in the system was initially determined using equation 5:

$$X_{TW} = 1 - \frac{M_{dry}}{M_{total}} \qquad (5)$$

where, X_{TW} is the total water content in the hydrogel, M_{dry} is the mass of the dried gel, and M_{total} is the mass of the swollen gel.

Following this, the amount of non-crystallisable water was calculated from equation 6:

$$X_{nc} = X_{tw} - (\frac{Q_{endo}}{Q_f}) \qquad (6)$$

where, X_{nc} is the fraction of non-crystallisable water, X_{tw} is the total water fraction of the gel, Q_{endo} is the heat of fusion of the crystallisable water as obtained from the DSC thermogram, and Q_f is the heat of fusion of free water (333 J/g).[37] It was assumed that the heat of fusion of crystallisable water in the gel was the same as that of ice. The total amount of water (X_{TW}) in the

system for the Ru5APS28 gel under immersion sorption conditions (h=0.454) was found to be 0.31. At this condition, the fractions of crystallisable (X_c) and non-crystallisable (X_{nc}) water were found to be 0.05 and 0.26, respectively. Therefore, from a representative Ru5APS28 gel sample with total swollen mass of 8.7 mg, there was 2.7 mg of water in total with 2.3 mg of non-crystallisable water occupying the hydrophilic sites and the remaining 0.4 mg being bulk crystallisable water. The amount of bound water present in the sample was calculated to be ~ 0.38 g water/g silk fibroin, which was less than that of rec1-resilin (~ 0.54) and was consistent with the lower level of hydrophilic amino acid residues present in silk fibroin.[14]

The effect of water content (h) on the T_g was predicted using the Fox-Flory equation:

$$\frac{1}{T_{g_{hs}}} = \frac{1-x_w}{T_{g_s}} + \frac{x_w}{T_{g_w}} \qquad (7)$$

where, T_{ghs} is the glass transition of hydrated silk fibroin, T_{gs} is the glass transition of dehydrated silk fibroin, and T_{gw} is the glass transition of quenched pure water (estimated as -135 ^oC).[38] Figure 5 inset shows the correlation between the experimentally measured T_g values and predicted T_g values of the Ru5APS28 sample with different levels of hydration using both vapour sorption and liquid water uptake. At the equilibrium h level (0.12 g water/g silk fibroin) under vapour sorption conditions, the T_g value (43 ^oC) closely agreed with the predicted value. However, when the water content was increased beyond this through immersion sorption the experimental values deviated negatively from the predicted values. A negative deviation is due to the presence of non-bound crystallisable water in addition to bound water. The presence of crystallisable water was also confirmed from the endothermic peak at 0 ^oC on the DSC thermogram, which was quantified. Thus, the presence of bound and non-bound water resulted in a decrease in the T_g to approximately -27.2 ^oC, which did not change when the h value increased above 0.2.

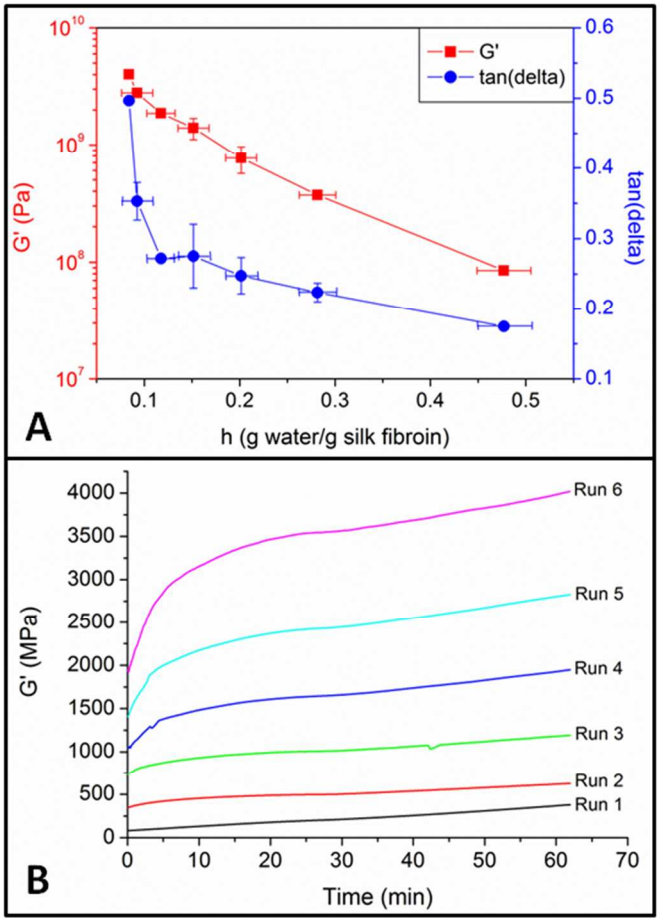

Figure 7. DMA results for Ru5APS28 samples with different hydration levels. A) G' and tan(delta). B) Change in G' with time for each DMA run.

Effect of hydration on the mechanical properties of silk fibroin gels

The effect of hydration on the mechanical properties of the crosslinked silk fibroin gels was examined using DMA with humidity accessory. The storage/loss moduli and tan delta values of the Ru5APS28 samples were measured using samples of rectangular geometry. It was observed that dry samples were too rigid for mounting and thus the samples were mounted after reaching equilibrium swelling in an immersion sorption system for 24 hours. During the run the humidity was ramped to 50 % and held for the duration of an hour with isothermal temperature, to prevent rapid dehydration of the system. The sample weight was measured at the beginning and end of

each run to determine the actual water content precisely. This was correlated to the measured modulus values (Figure 7A) and the curves generated for each run are shown in Figure 7B, where run 1 is the experiment with the equilibrium-swollen gel progressing to run 7 when the gel has the lowest h value. From the graph it can be observed that G' increased as the samples dried and less water was present in this sample. At the highest h value (= 0.454 g water/g silk fibroin), G' had a value of 81 MPa, whilst at lower h values (h = 0.08 g water/g silk fibroin) G' increased to a maximum of 4000 MPa. Thus, the presence of water affected the mechanical properties greatly, with higher water content resulting in an increase in the molecular mobility of the silk fibroin gels and loss of water leading to increased stiffness (higher G'). This has been also confirmed by the DSC experiments where the T_g becomes lower with higher water content. The water acts as a plasticiser to increase the flexibility and extensibility.[20] Dehydrated regenerated silk fibroin films prepared by Motta et al. showed storage moduli of 1834 MPa and 903 MPa at 0 ^{o}C and 37 ^{o}C, respectively.[39] The authors also prepared films, which were treated overnight with methanol and high temperatures to induce physical crosslinking through β-sheet formation.[39] The storage moduli for the dehydrated methanol treated films were 2760 MPa and 2445 MPa at 0 ^{o}C and 37 ^{o}C, respectively.[39] Whilst the values for the heat treated films were 4840 MPa and 4410 MPa at 0 ^{o}C and 37 ^{o}C, respectively. The increase in crystalline content was shown to result in increasing stiffness, with highest values due to high amount of physically crosslinked films due to heat treatment.[39] The uncrosslinked film displayed a significantly lower G' value than the crosslinked gel. In addition, the heat treated samples showed comparable values to our dehydrated gels, whilst methanol treatment resulted in materials with slightly less stiffness. Therefore, ruthenium-mediated photo-crosslinking of silk fibroin is a highly suitable and facile method for the rapid preparation of hydrogels with high strength, the elasticity of which may be tuned through the moisture content as shown here.

Structural analysis of silk fibroin powder, films, and gels

As the extent of silk crosslinking did not change very much using the ruthenium-mediated process with the variables such as time and concentration; we have hypothesised that the nano-structure may be a contributing factor. From the amino acid sequence, it can be observed that the majority of the tyrosine residues reside in the crystalline regions of the silk fibroin sequence.[39] However, on dissolution in water, the tyrosine residue is expected to be exposed to the surface of the protein and air-water interface and hence become accessible for crosslinking. Such rearrangement of fibroin chain in water is necessary for the tyrosine residues to participate in crosslinking. The silk particles that are removed via filtration of the solutions are attributed to the ordered rigid β sheet structure comprising of alanine residues that are insoluble. The dry silk fibroin may also have β sheet structure, which has been indicated through DSC experiments. If a fixed fraction of silk is removed during the filtration step, this would explain why the same amount of silk is crosslinked regardless of the conditions. In addition, the flexibility of the gel is attributed to the amorphous and less ordered hydrophilic glycine rich portion of the silk being involved in the tyrosine mediated crosslinking reaction. Photo-acoustic Fourier transform infrared (PA-FTIR) spectroscopy was used to analyse the structural changes of the initial silk fibroin powder, film prepared from filtered solution, and the Ru5APS28 gel prepared from filtered solution that occurred during the different processing steps.

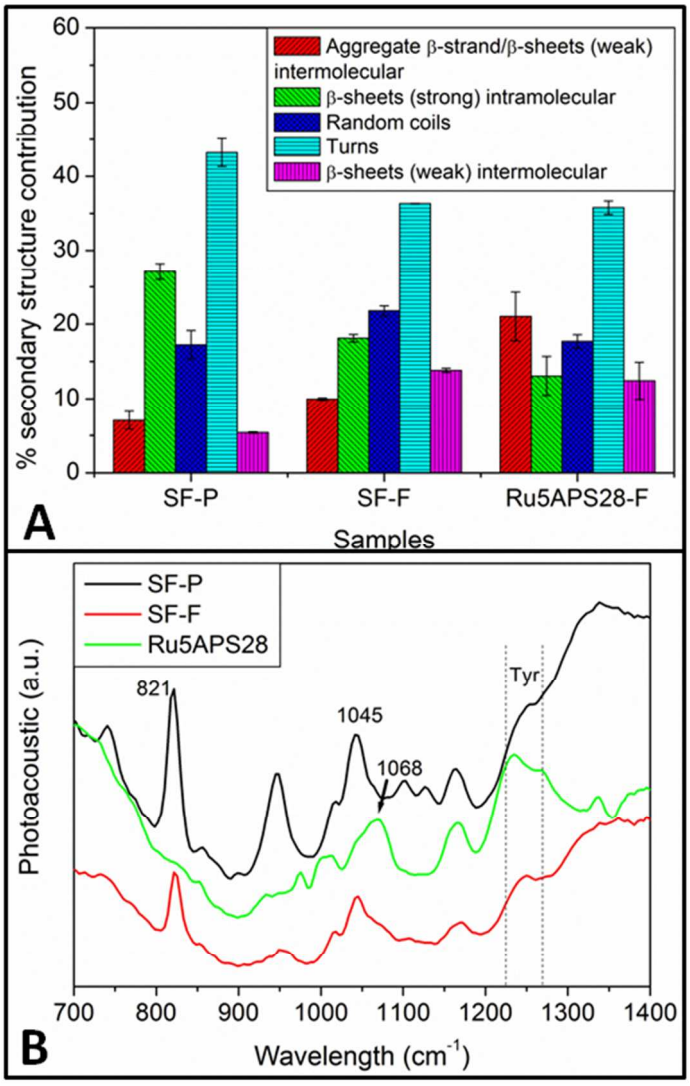

Figure 8. A) Secondary structure content of silk fibroin powder, film and Ru5APS28 gel as calculated from PA-FTIR data. (B) FTIR spectra of different forms of silk fibroin. SF-P: silk fibroin powder; SF-F: silk film from filtered solution; Ru5APS28-F: silk gel from filtered solution).

The secondary structure content of the silk fibroin powder, film, and gel was examined using PA-FTIR spectroscopy. The spectra of the samples show the presence of various amide bands corresponding to a number of conformations. Two distinct conformation bands with peak maxima between 1700-1600 cm^{-1} (due to amide I) and between 1600-1500 cm^{-1} (due to amide II)

are observed in the spectra. The amide I band was deconvoluted using the Magic Plot software by applying Gaussian curve fitting to this region (1600 – 1700 cm^{-1}).[22,30] The areas under the peaks were determined and the proportion of each secondary structure was calculated from this information to give a semi-quantitative comparison between the samples. Figure 8A shows the secondary structure content for the samples at different conditions. The beta-sheet content of the powder was calculated from the peak position at 1628 – 1637 cm^{-1} and was found to be27 ± 1%.[22,30] Whereas, the films from the filtered solution had a beta-sheet contribution of 18 ± 0.5%. In addition, the Ru5APS28 gel from filtered solutions displayed the lowest beta-sheet contributions of 13 ± 3%. Therefore, there was a significant decrease (~10%) in the beta-sheet content from the powder to the Ru5APS28 gel form. It has been reported earlier that the beta-sheet crystalline structure (silk II) contributes to the rigidity of *B. mori* silk fibroin.[30] Therefore, the decrease in beta-sheet content is consistent with our hypothesis that the gels contained less ordered silk fibroin when crosslinked.

The PA-FTIR spectra were also examined to confirm the presence of di-/trityrosine crosslinks upon gelation of the silk solutions. There were a number of differences detected between the spectra of the powder and the film to the spectra of the gels in the region of 700 – 1400 cm^{-1} (Figure 8B). The strong band at ~821 cm^{-1} in the spectra of the powder and films was assigned to tyrosine as it is in the region of para-disubstituted benzenes (800 – 860 cm^{-1}). However, it was observed that this peak was not present in the spectra of the Ru5APS28 gels, which confirms the crosslinking of tyrosine. In addition, the region from 1170 to 1270 cm^{-1} that is attributed to tyrosine differed between the spectra of the powder and film to the gel.[41] The spectra of the powder and film showed an increase in intensity in this region, however in the gel spectra there was a decrease, indicating a decrease in the presence of tyrosine. Furthermore, a shift in the

region of the aliphatic amines (1020 – 1220 cm^{-1}) for the spectra of the gel when compared to the powder and film indicates changes in the structure on the formation of hydrogels.

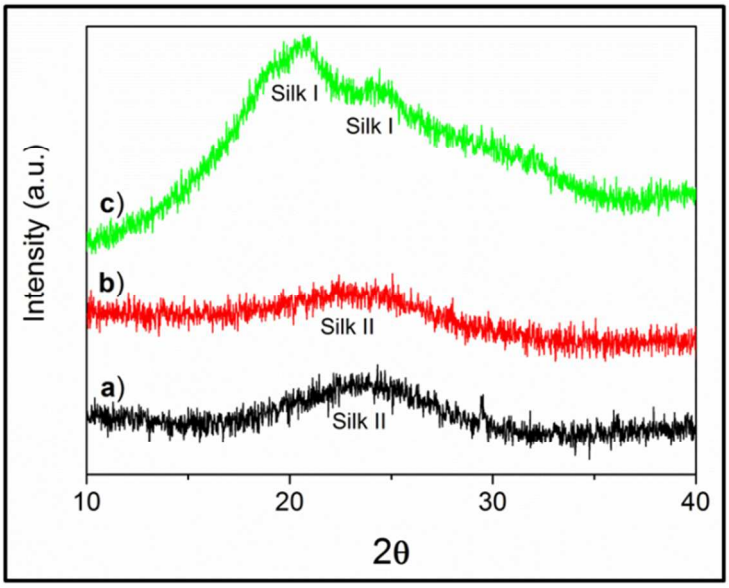

Figure 9. X-ray diffractograms of a) silk powder; b) silk film from filtered solution; c) Ru5APS28 gel from filtered solution.

XRD experiments were employed to give further information on the nano-structural organisation of the silk fibroin powder, film, and the Ru5APS28 gel. Figure 9 shows the X-ray diffractograms for the aforementioned samples. The d spacings for the main peaks were determined and compared to literature values to obtain information about the structure of the silk fibroin in the different states. The silk powder and film show broad spectra with peaks centred at 23.6 and 23.5°, which correspond to d spacing of ~3.8 Å. From literature, a d spacing of 3.8 Å has been associated with silk II structure (crystalline beta-sheet).[42] However, as the peaks are so broad and have a low intensity, it is expected that a range of silk I and silk II conformations exist for the silk powder and filtered film. The diffractogram for the Ru5APS28 gel prepared from the filtered solution shows much more intense peaks at 20.4 and 24.4°, which correspond to d spacing values of 4.4 and 3.6 Å. These d spacings have been attributed to the silk I structure

(type II beta-turn), which is the hydrated form.[20,43] Therefore, the silk gels contain the hydrated silk I structure, which allows for the uptake of water. The XRD results correlate with the DSC and PA-FTIR results in that the silk undergoes structural changes from containing more crystalline component in the powder and films to more amorphous when crosslinked to form hydrogels. A summary of the structural information obtained for the different forms of the silk fibroin can be found in Table 3.

Table 3. Summary of structural information determined through different experimental methods.

Experimental method	BMWS powder	BMWS film from filtered solution	BMWS gel from filtered solution
DSC	Silk II (crystalline)	Predominantly Silk I (amorphous)	Silk I (amorphous)
PA-FTIR	Silk II (crystalline) with some Silk I (amorphous)	Silk I (amorphous) with some silk II (crystalline)	Predominantly silk I (amorphous)
XRD	Predominantly silk II (crystalline) with some Silk I (amorphous)	Silk II (crystalline) with some Silk I (amorphous)	Silk I (amorphous)

Growth of ATDC5 cells on silk fibroin hydrogels

A representative silk fibroin hydrogel (Ru5APS28) was evaluated for its capacity to support cell growth *in vitro*. The pre-chondrocyte cell line ATDC5 was chosen to study the biocompatibility of the hydrogels, as these gels could be suitable for invertebral disc replacement applications due to the high modulus as determined by DMA. The adhesion and proliferation of the ATDC5 cells, seeded at a density of 12 x 10^4 cells/cm^2, was assessed using phase-contrast microscopy. Figure 10a and b shows the morphological characteristics of ATDC5 cells cultured overnight on both TCP and silk fibroin hydrogel, respectively. As seen in Figure 10a and b, the cells cultured on both TCP and silk fibroin hydrogel displayed a characteristic spread, adherent, elongated morphology. Furthermore, ATDC5 viability and proliferation on the Ru5APS28 hydrogels was

assessed over a period of 7 days and cell proliferation evaluated using the tetrazolium salt, WST-1 [2-(4-iodophenyl)-3-(4-nitrophenyl)-5-(2,4-disulfophenyl)-2H-tetrazolium]. As seen in Figure 10c, the ATDC5s remained viable and expanded in cell number throughout the culture period. However, it should be noted that the ATDC5 cells displayed reduced proliferative capacity (p value < 0.0001) on the hydrogels compared to the TCP, at each time point examined. These findings indicate that the silk fibroin photo-crosslinked hydrogels are non-toxic *in vitro*, support cell attachment and cell proliferation and represent promising, biocompatible biomaterials for tissue engineering applications.

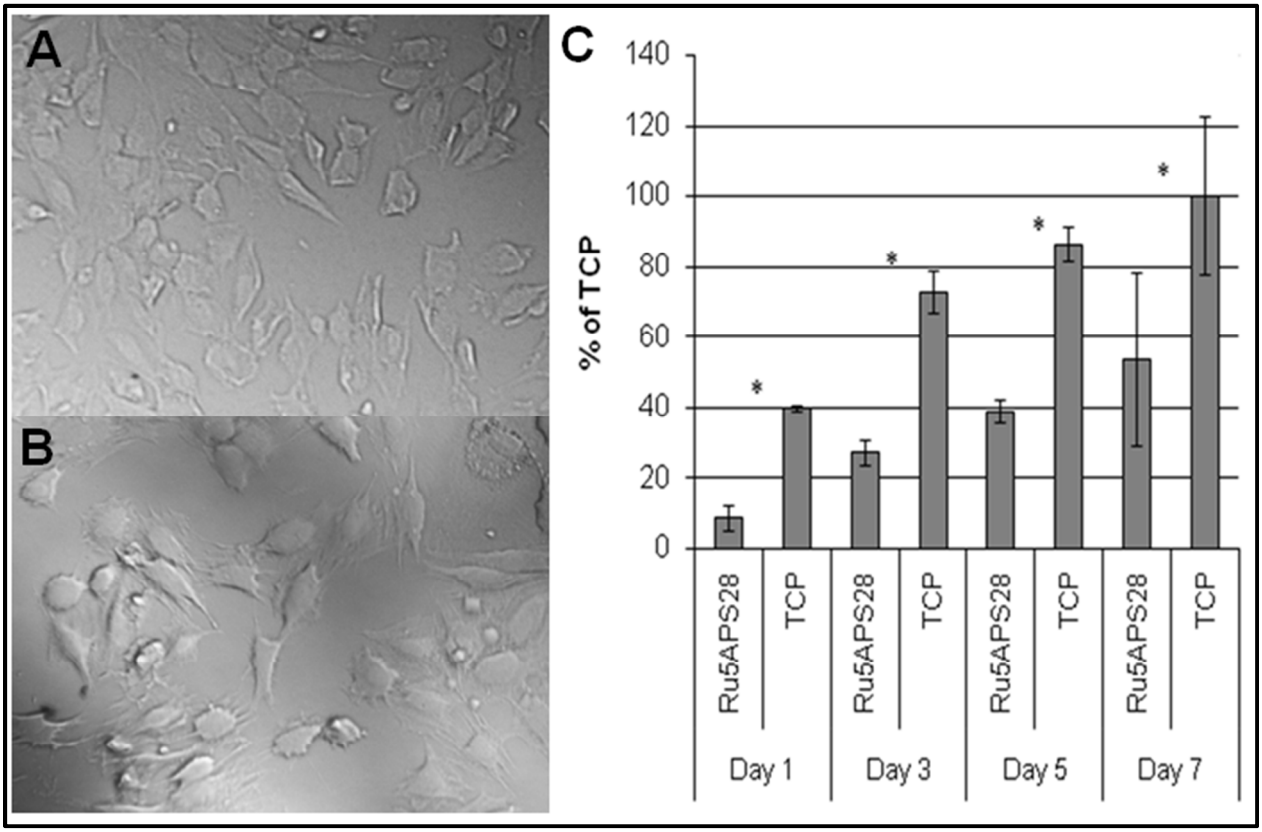

Figure 10. Phase-contrast micrographs of growth of ATDC5 cells after overnight culture on A) TCP and B) Ru5APS28 hydrogel. C) ATDC5 cell proliferation as assessed using a WST-1 proliferation assay. * Represents groups that are statistically different (P value < 0.05).

Conclusions

In summary, for the first time we have demonstrated successful photo-crosslinking of *B.mori* silk fibroin with Ru(II)$(bpy)_3^{2+}$ as the catalyst and APS as the electron acceptor. The extent of crosslinking depends on the accessibility/availability of the tyrosine residue in the amorphous region to participate in the crosslinking reaction. This has been confirmed through DSC, PA-FTIR, and XRD studies, which show that the gels are less rigid and contain less beta-sheet content than the original silk. In addition, water/moisture has been shown to play a significant role on the molecular chain dynamics. The presence of both crystallisable and non-crystallisable water resulted in a plasticised Ru5APS28 silk fibroin gel at room temperature. In addition, water/moisture was also observed to play an important role in tuning the mechanical properties of the Ru5APS28 gel. The storage modulus (G') values were tuned from 4000 MPa to 81 MPa with hydration levels (h) of 0.08 and 0.454, respectively. The effect of water/moisture on the chain dynamics and mechanical properties is important for understanding the performance of the hydrogel under different conditions. Thus, we have developed a route for in-situ photo-crosslinking of silk fibroin to form hydrogels with tuneable modulus values. We have shown through cell culture studies that the hydrogels support the attachment and growth of pre-chondrocyte cells, highlighting their potential suitability as biomaterials for tissue engineering applications.

Acknowledgements

This research has been financially supported by the Australian Research Council (ARC) through Discovery Grant funding.

Electronic Supplementary Information (ESI) available: [This includes the NMR data confirming the identity of the silk powder, the full crosslinking reaction schematic, fluorescence and UV-vis spectra of the gels, and determination of the minimum Ru(II)$(bpy)_3^{2+}$ concentration required for crosslinking]. See DOI: 10.1039/b000000x/

References

1. J. Kundu, L. A. Poole-Warren, P. Martens, S. C. Kundu, *Acta Biomater.,* 2012, **8**, 1720.

2. A. Alessandrino, B. Marelli, C. Arosio, S. Fare, M. C. Tanzi, G. Freddi, *Eng. Life Sci.,* 2008**, 8**, 219-225.

3. B. –M. Min, G. Lee, S. H. Kim, Y. S. Nam, T. S. Lee, W. H. Park, *Biomaterials,* 2004, **25**, 1289-1297.

4. J. A. Werkmeister, J. A. M. Ramshaw, *Biomed. Mater.,* 2012, **7**, 012002.

5. S. Aznar-Cervantes, M. I. Roca, J. G. Martinez, L. Meseguer-Olmo, J. L. Cenis, J. M. Moraleda, T. F. Otero, *Bioelectrochemistry,* 2012, **85**, 36-43.

6. A. Matsumoto, J. Chen, A. L. Collette, U.-J. Kim, G. H. Altman, P. Cebe, D. L. Kaplan, *J. Phys. Chem. B,* 2006, **110**, 21630.

7. S. Nagarkar, T. Nicolai, C. Chassenieux, A. Lele, *Phys. Chem. Chem. Phys.,* 2010, **12**, 3834.

8. C. Vepari, D. L. Kaplan, *Prog. in Polym. Sci.,* 2007, ***32***, 991-1007.

9. Q. Lu, Y. Huang, M. Li, B. Zuo, S. Lu, J. Wang, H. Zhu, D. L. Kaplan, *Acta Biomater.,* 2011, **7**, 2394-2400.

10. N. Kojic, M. J. Panzer, G. G. Leisk, W. K. Raja, M. Kojic, D. L. Kaplan, *Soft Matter,* 2012, **8**, 2897-2905.

11. A. Vasconcelos, A. C. Gomes, A. Cavaco-Paulo, *Acta Biomater.,* 2012, **8**, 3049.

12. S. S. Silva, D. Maniglio, A. Motta, J. F. Mano, R. L. Reis, C. Migliaresi, *Macromol. Biosci.,* 2008, **8**, 766-774.

13. G. Kang, K. Lee, C. Ki, Y. Park, *Fiber Polym.,* 2004, **5**, 234-238.

14. M. Y. Truong, N. K. Dutta, N. R. Choudhury, M. Kim, C. M. Elvin, K. M. Nairn, A. J. Hill, *Biomaterials,* 2011, **32**, 8462-8473.

15. K. Schacht, T. Scheibel, *Biomacromolecules,* 2011, **12**, 2488.

16. M. Mondal, K. Trivedy, S. Nirmal Kumar, *Caspian J. of Enviro. Sci.,* 2007, **5**, 63-76.

17. C. M. Elvin, T. Vuocolo, A. G. Brownlee, L. Sando, M. G. Huson, N. E. Liyou, P. R. Stockwell, R. E. Lyons, M. Kim, G. A. Edwards, G. Johnson, G. A. McFarland, J. A. M. Ramshaw, J. A. Werkmeister, *Biomaterials,* 2010, **31**, 8323-8331.

18. J. Ishikuro, Y.Hirai, T. Nakajima, *Sen'i Gakkaishi,* 1994, **50**, 28-31.

19. S. Fossey, D. Kaplan, In *Polymer Data Handbook*, Oxford University Press, Inc., 1999.

20. C. Zhang, D. Song, Q. Lu, X. Hu, D. L. Kaplan, H. Zhu, *Biomacromolecules,* 2012, **13**, 2148-2153.

21. X. Hu, X Wang, J. Rnjak, A. S. Weiss, D. L. Kaplan, *Biomaterials,* 2010, **31**, 8121-8131.

22. S. Lin, G. Lu, S. Liu, S. Bai, X. Liu, Q. Lu, B. Zuo, D. L. Kaplan, H. Zhu, *J. Mater. Chem. B,* 2014, **2**, 2622-2633.

23. Shukunami, Y. Ohta, M. Sakuda, Y. Hiraki, *Exp. Cell. Res.,* 1998, **241**, 1-11.

24. C. Shukunami, K. Ishizeki, T. Atsumi, Y. Ohta, F. Suzuki, Y. Hiraki, *J. Bone & Min. Res.,* 1997, **12**, 1174-1188.

25. K. Vandyke, S. Fitter, A. C. W. Zannettino, *Blood Cancer Journal,* 2011, **1**, e2; doi:10.1038/bcj.2011.1.

26. S. Fitter, K. Vandyke, S. Gronthos, A. C. W. Zannettino, *J. Mol. Endocrinol.,* 2012, **48**, 229-240.

27. W. Xiao, W. Liu, J. Sun, X. Dan, D. Wei, H. Fan, *J. Bioact. Compat. Polym.,* **27**, 327-341.

28. S. Van Vlierberghe, P. Dubruel, E. Lippens, M. Cornelissen, E. Schacht, *J. Biomater. Sci. Polym. Ed.,* 2009, **20**, 1417-1438.

29. F. Ganji, S. Vasheghani-Farahani, E. Vasheghani-Farahani, *Iranian. Polym. Journal*, 2010, **19**, 375-398.

30. X. Hu, D. Kaplan, P. Cebe, *Macromolecules,* 2006, **39**, 6161-6170.

31. S. Rauscher, R. Pomès, In *Fuzziness*; M. Fuxreiter, P. Tompa, Eds.; Springer US: 2012, **725**, 159-183.

32. M. Martino, T. Perri, A. M. Tamburro, *Macromol. Biosci.,* 2002, **2**, 319-328.

33. F. Teulé, B. Addison, A. R. Cooper, J. Ayon, R. W. Henning, C. J. Benmore, G. P. Holland, J. L. Yarger, R. V. Lewis, *Biopolymers,* 2012, **97**, 418-431.

34. M. Kim, S. Tang, B. D. Olsen, *J. Polym. Sci. Part B: Polym. Phys.,* 2013, **51**, 587-601.

35. Y. Zhou, S. Wu, V. P. Conticello, *Biomacromolecules,* 2001, **2**, 111-125.

36. N. Agarwal, D. A. Hoagland, R. J. Farris, *J. Appl. Poly. Sci.,*1997, **63**, 401-410.

37. T. Wang, S. Gunasekaran, *J. Appl. Poly. Sci.,* 2006, **101**, 3227-3232.

38. V. Velikov, S. Borick, C. A. Angell, *Science,* 2001, **294**, 2335-2338.

39. A. Motta, L. Fambri, C. Migliaresi, *Macromol. Chem. and Phys.,* 2002, **203**, 1658-1665.

40. C. Z. Zhou, F. Confalonieri, M. Jacquet, R. Perasso, Z. G. Li, J. Janin, *Proteins: Struct., Funct., Bioinf.,* 2001, **44**, 119-122.

41. A. Barth, *Prog. Bio. Mol. Biol.,* 2000, **74**, 141-73.

42. I. C. Um, H. Y. Kweon,Y. H. Park, S. Hudson, *Int. J. Biol. Macromol.,* 2001, **29**, 91-97.

43. H.-J. Jin, *Nature,* 2003, **424**, 1057-1061.